Organic & Biomolecular Chemistry

Cite this: *Org. Biomol. Chem.*, 2011, **9**, 4168

www.rsc.org/obc

PAPER

Polyethylene glycol-functionalized benzylidene cyclopentanone dyes for two-photon excited photodynamic therapy†

Yuxia Zhao,[a] Weijia Wang,[a,c] Feipeng Wu,*[a] Yang Zhou,[b] Naiyan Huang,[b] Ying Gu,[b] Qianli Zou[a,c] and Wei Yang[a,c]

Received 31st December 2010, Accepted 10th March 2011
DOI: 10.1039/c0ob01278e

A series of polyethylene glycol-functionalized benzylidene cyclopentanone dyes with varying lipid/water partition coefficients were synthesized in high yields by a simple process. Detailed characterization and systematic studies of these molecules, including linear and nonlinear photophysical properties, reactive oxygen yields, and *in vitro* photodynamic therapy (PDT) activities, were conducted. Four of these dyes exhibited good solubility in PBS (>2 mg ml^{-1}, which is sufficient for clinical venous injection), high reactive oxygen yields, large two-photon absorption and low dark toxicity, under the therapy dosage. Among them, two dyes could be absorbed efficiently by human rectal cancer 1116 cells, and presented strong two-photon excited PDT activity in *in vitro* cell experiments.

Introduction

Photodynamic therapy (PDT), a promising noninvasive treatment for cancer and nonmalignant tumors, has been used in clinical treatment for a long period. Its mechanism is using light to activate a tumor-localized photosensitizer, selectively to destroy tumor tissue *via* the *in situ* generation of highly cytotoxic reactive oxygen species (ROS), for example singlet oxygen ($^1O_2$) or superoxide anion radical ($O_2^{-\bullet}$).[1] Compared to other cancer treatment modalities, such as surgery, radio- and chemo-therapy, PDT has advantages of high selectivity to malignant target *vs*. normal cells, and low damage.[2] However, due to the limited tissue penetration, its applications are mainly confined to superficial tissues of an organ, such as in esophageal cancer and skin disease.[3] Two-photon excited PDT (TPE-PDT) has attracted much attention in recent years for its significant benefit of deep tissue penetration due to the fact that two photons of infrared light rather than one photon of visible light are absorbed by photosensitizer,[4,5] which helps to resolve the penetration problem mentioned above, in present PDT. Furthermore, the quadratic dependence of two-photon excitation on the laser intensity restricts excitation to the focus of a laser beam, which allows the generation of cytotoxic ROS to be confined to a small volume, reducing collateral damage to normal tissues. Therefore, the spatial selectivity and accuracy of the treatment could be further enhanced.[6]

Conventional clinical PDT drugs were used as photosensitizers in early TPE-PDT studies, such as Photofrin and Verteprofin.[6,7] However, their two-photon absorption cross-section (σ) values are too small (for example, the σ value of Photofrin is 7.4 GM[6] at 850 nm and the σ value of Verteprofin is 51 GM[7] at 900 nm, 1 GM = 10^{-50} cm^4 s molecule^{-1} photon^{-1}) to be suitable clinically because their dynamic power ranges for PDT (the ratio of the threshold for photothermal or photomechanical damage *vs.* the lowest light intensities required for a clear therapeutic effect) are not large enough. For exploring the full potential of TPE-PDT, recently various design strategies have been employed to synthesize water-soluble photosensitizers with large two-photon absorption (TPA) cross-section and evident photodynamic activity.[8–13] Among them, porphyrin dimer derivatives[8] have been progressed to *in vivo* testing and proved the TPE-PDT effect by selectively closing blood vessels. Moreover, other valuable approaches such as encapsulation of TPA photosensitizer into water-dispersed nanoparticles or encapsulation of photosensitizer into amphiphilic TPA-chromophore-containing block copolymers have been reported to successfully induce a TPE phototoxic effect in *in vitro* cell testing.[14,15] These exciting results have attracted lots of attention for TPE-PDT, however, for realizing its practical application, much more systematic work is still required.

In our previous work, benzylidene cyclopentanone dyes were found to have large σ values (400–3300 GM around 800 nm, which were comparatively high based on their simple molecular structures), and high photosensitizing efficiencies.[16–18] Unfortunately, these dyes are all hydrophobic. In this work, we introduced a number of low molecular weight polyethylene glycol (PEG)

[a]*Technical Institute of Physics and Chemistry, Chinese Academy of Sciences, Beijing, 100190, P. R. China. E-mail: fpwu@mail.ipc.ac.cn*
[b]*Department of Laser Medicine, Chinese PLA General Hospital, Beijing, 100853, P. R. China*
[c]*Graduate University of Chinese Academy of Science, Beijing, 100049, P. R. China*

† Electronic supplementary information (ESI) available: ^{1}H and ^{13}C NMR spectra of all target dyes. See DOI: 10.1039/c0ob01278e

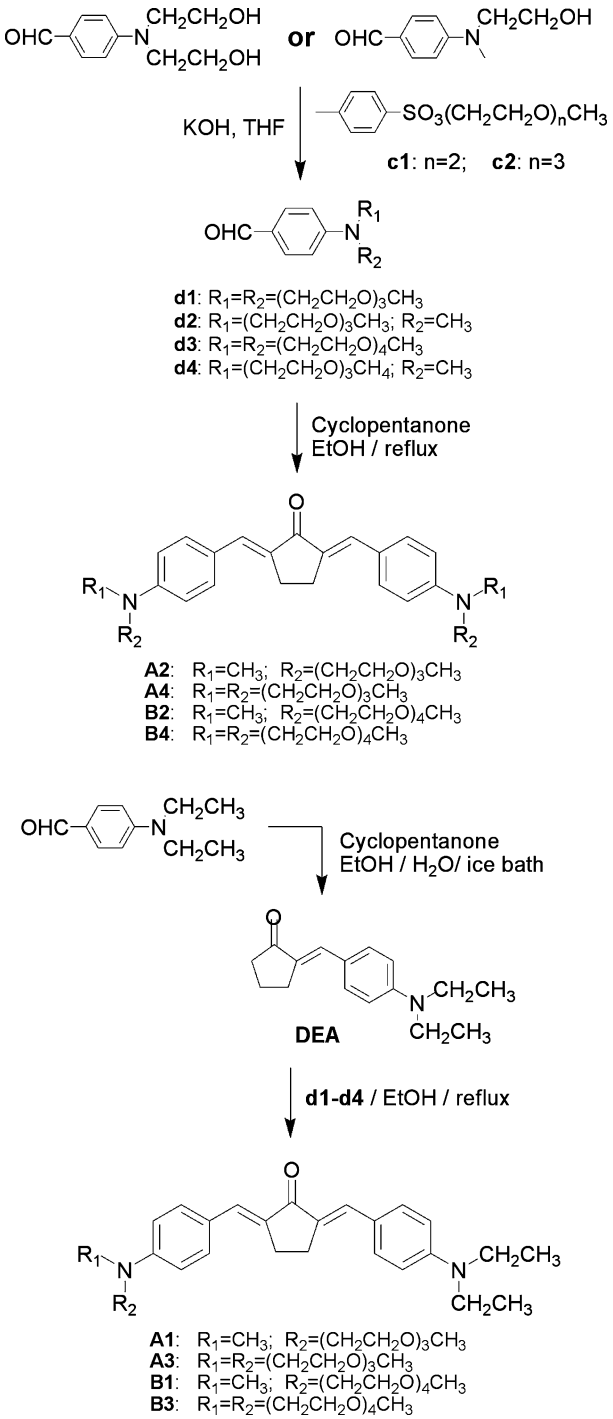

Scheme 1 Synthesis of dyes **A1**–**B4**.

chains into the benzylidene cyclopentanone core (Scheme 1) to improve their solubility in biological media and to optimize their lipid/water partition coefficients (PC) through adjusting the length and number of PEG chains covalently linked to the dyes. After systematic studies of their water-solubility, linear and non-linear photophysical properties, and PDT activities, two dyes successfully demonstrated their PDT and TPE-PDT application potential in *in vitro* cell testing.

Table 1 Solubility in PBS and lipid/water (octanol/water) partition coefficient (PC) of dyes

Compound	Solubility in PBS/mg mL^{-1}	log PC
A1	—	>8
A2	0.0194	>7
A3	0.0035	>7
A4	4.6	2.57
B1	—	>8
B2	2.8	2.99
B3	2.6	3.04
B4	5.3	2.32

Results and discussion

Synthetic strategy

The new series of dyes presented in this study were obtained by a simple two-step synthesis process illustrated in Scheme 1. The prototype dye is 2,5-bis[4-(diethylamino)benzylidene]cyclopentanone (**BDEA**), which is insoluble in aqueous media. Therefore, we introduce amphiphilic ethylene glycol moieties, which are known for conferring cell permeability and tumor targeting characteristics on photosensitizers,[19–21] into the parent structure. Intermediate products **d1–d4** were prepared by substitution reaction between 4-[bis(2-hydroxyethyl)amino]-benzaldehyde or 4-[(2-hydroxyethyl)methylamino]benzaldehyde and 1-(*p*-tolysulfonyl)-3,6-dioxoheptane (**c1**) or 1-(*p*-tolysulfonyl)-3,6,9-trioxodecane (**c2**) in high yields (72–79%). Target dyes **A1–B4** were synthesized by base-catalyzed condensation of aromatic aldehydes **d1–d4** with cyclopentanone or 2-[4-(diethylamino)benzylidene]cyclopentanone (**DEA**) and purified by column chromatography on silica in good yields (61%–74%).

Solubility and lipid-water partition coefficient (PC)

As shown by the data in Table 1, four dyes (**A4**, **B2**, **B3** and **B4**) exhibit good water solubility in the range of 2.6–5.3 mg ml^{-1} in PBS (pH = 7.4), while dyes **A2** and **A3** are only slightly soluble, and dyes **A1** and **B1** are almost insoluble. This shows that increasing the number of PEG chains or extending their length leads to increase of solubility in PBS.

In PDT, photosensitizers are injected into a vein and transported to target tumor tissues through the blood circulating system, and enter tumor cells and intercellular regions through the lipid membranes of blood vessels and cells, which requires the photosensitizers to be both water- and lipid-soluble. Thus a moderate lipid/water PC is important for a PDT photosensitizer.[22,23] The results show that the lipid/water (octanol/water) PC values of dyes **A1–A3** and **B1** are very large (log PC >7), with almost all dye in the organic phase, while **A4** and **B2–B4** have moderate lipid/water PC values. For ensuring sufficient cellular uptake of dyes, an appropriate PC value is required, *i.e.* a fair degree of water solubility, as shown by dyes **A4** and **B2–B4**.

One- and two-photon photophysical properties

The UV-Vis absorption spectra as well as one-photon excited fluorescence emission spectra excited at 480 nm of all dyes in *n*-octanol are almost exactly the same, as shown in Fig. 1A and Table 2, which proves that the terminal PEG chains have almost no effect

Table 2 One- and two-photon photophysical properties of new dyes[a]

Compound	Solvent	λ_{max}^{abs}/nm	$10^4\varepsilon_{max}$/M^{-1} cm^{-1}	λ_{max}^{fl}/nm	Φ_f	Φ_Δ[b]	Φ_Δ[c]	σ_{max}/GM
A1	*n*-Octanol	486	6.3	578	0.30	0.22	0.24	869
A2	*n*-Octanol	486	6.2	578	0.28	0.20	0.27	814
	PBS	505	4.7	636	0.028	—	—	—
A3	*n*-Octanol	486	6.1	577	0.27	0.19	0.26	861
A4	*n*-Octanol	488	6.2	578	0.29	0.18	0.24	986
	PBS	507	4.8	636	0.023	—	—	—
B1	*n*-Octanol	486	6.2	578	0.28	0.21	0.23	783
B2	*n*-Octanol	487	6.3	578	0.29	0.20	0.30	781
	PBS	508	5.0	637	0.019	—	—	—
B3	*n*-Octanol	487	6.1	578	0.28	0.21	0.22	917
	PBS	511	4.5	636	0.026	—	—	—
B4	*n*-Octanol	486	6.0	578	0.29	0.18	0.26	990
	PBS	509	5.1	636	0.02	—	—	—
BDEA	*n*-Octanol	490	6.8	578	0.21	0.23	0.28	1052

[a] λ_{max}^{abs} is one-photon absorption band-maximum; ε_{max} is molar absorption coefficient at λ_{max}^{abs}; λ_{max}^{fl} is fluorescence band maximum; Φ_f is fluorescence quantum yield; Φ_Δ is singlet oxygen quantum yield. [b] Measured by photochemical trap method, [c] Measured by $^1O_2$ phosphorescence intensity; σ_{max} is the maximum TPA cross section obtained within 720–880 nm.

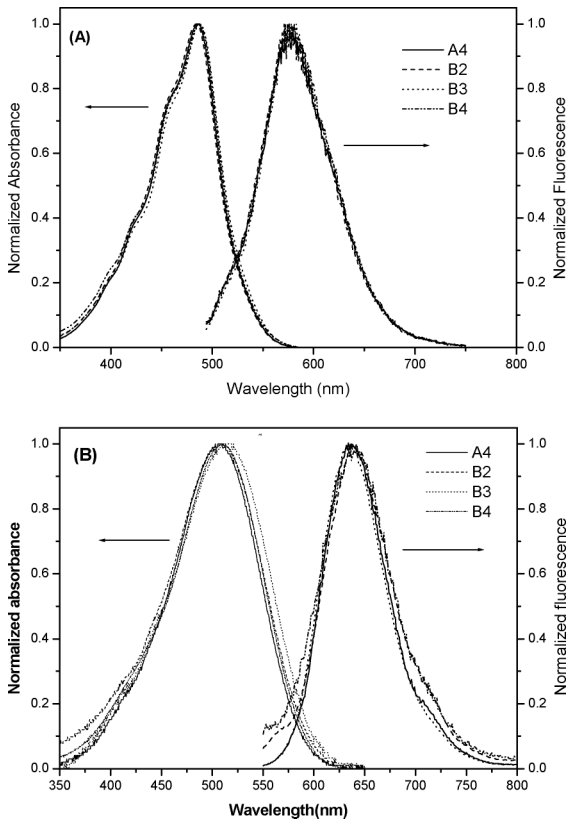

Fig. 1 Normalized absorption and one-photon excited fluorescence emission spectra of water-soluble dyes in *n*-octanol (A), excited at 480 nm, and in PBS (B), excited at 530 nm.

on the electron transition of the benzylidene cyclopentanone core. The absorption and one-photon excited fluorescence emission spectra excited at 530 nm (Fig. 1B) of water-soluble **A4** and **B2–B4** in PBS (PH = 7.4) are also very similar.

The two-photon excitation (TPE) spectra of all dyes within the range 720–880 nm were measured using the TPE fluorescence technique with a mode-locked Tsunami Ti : sapphire femtosecond laser (80 MHz, <130 fs). Their maxima σ values (σ_{max}) appear at 840 nm in the range of 780–990 GM (shown in Fig. 2), which is comparable with the 1052 GM of BDEA (without PEG chains), indicating that the terminal PEG chains have little effect on the TPA characterization of the benzylidene cyclopentanone core.

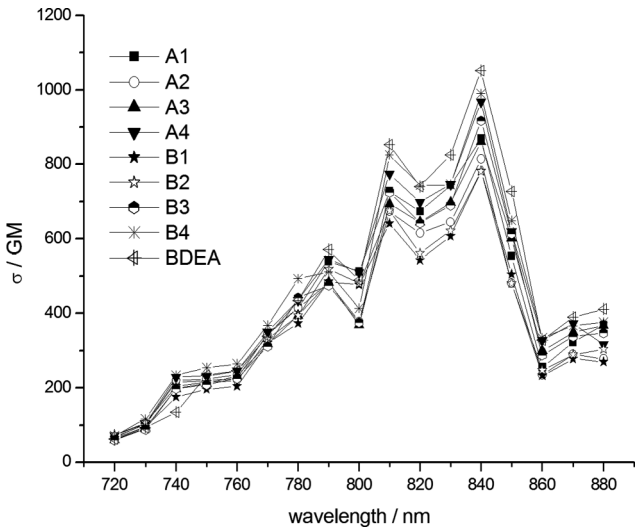

Fig. 2 Two-photon excitation spectra of dyes in *n*-octanol. The exciting source is a mode-locked Tsunami Ti : sapphire laser (720–880 nm, 80 MHz, <130 fs).

Photosensitization activity

By irradiating oxygen-saturated solutions of **A4** and **B2–B4** with a 532 nm laser in the presence of DMPO used as superoxide radical ($O_2^{-\bullet}$) spin-trapping reagent or TEMP used as a singlet oxygen ($^1O_2$) spin-trapping reagent, an electron paramagnetic resonance (EPR) signal appeared (inset in Fig. 4) with a *g* factor and hyperfine coupling constants (g = 2.0056, α^N = 12.48 G, α_β^H = 10.36 G, α_γ^H = 1.35 G) in good agreement with those for a DMPO–$O_2^{-\bullet}$ adduct,[24] or (inset in Fig. 3) with triplet peaks in equal intensity (g = 2.0056, α^N = 16.3 G) due to the TEMP–$^1O_2$ adduct.[24] The results confirm that both $O_2^{-\bullet}$ and $^1O_2$ species can be generated by **A4** and **B2–B4** under 532 nm illumination. In

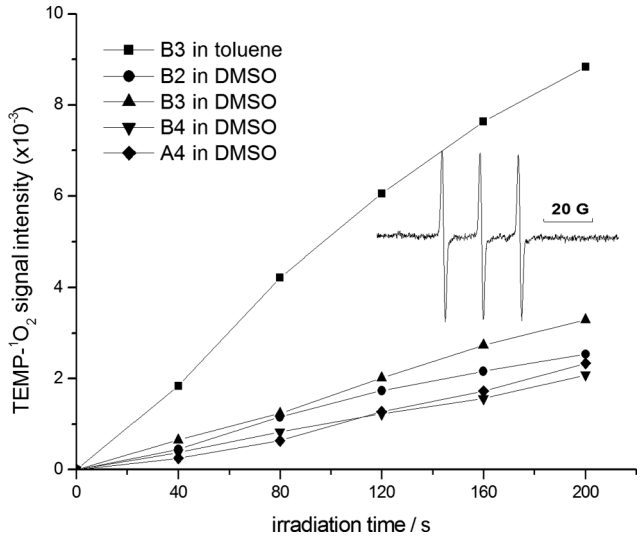

Fig. 3 EPR signal intensity of TEMP–$^1O_2$ adducts as a function of irradiation time (irradiated at 532 nm) for oxygen-saturated DMSO and toluene solutions of dyes (1×10^{-4} M). Inset: The EPR spectrum of TEMP–$^1O_2$ adduct.

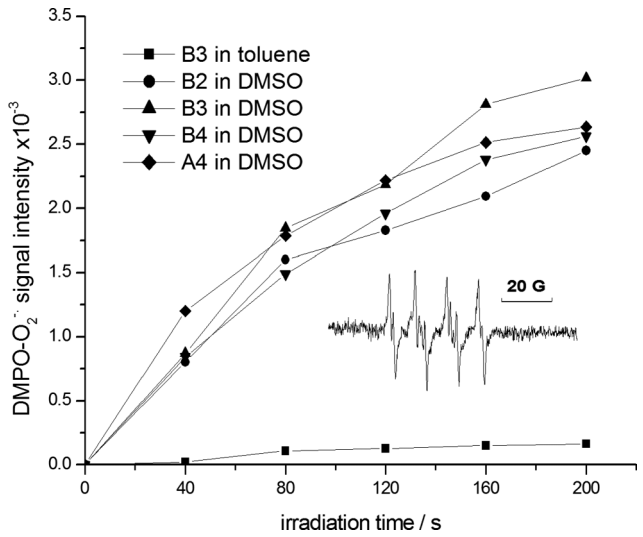

Fig. 4 EPR signal intensity of DMPO–$O_2^{-\bullet}$ adducts as a function of irradiation time (irradiated at 532 nm) for oxygen-saturated DMSO and toluene solutions of dyes (1×10^{-4} M). Inset: The EPR spectrum of DMPO–$O_2^{-\bullet}$ adduct.

addition, the efficiency to generate reactive oxygen species (ROS) depends significantly on the solution environment. For example, for **B3** the polar solvent DMSO facilitates the production of $O_2^{-\bullet}$ while the nonpolar solvent toluene facilitates the production of $^1O_2$. Dependences of EPR signal intensity on irradiation time of the four dyes are also shown in Fig. 3 and 4 and it is clear that the four dyes have similar photosensitization activity. Among them, **B3** is relatively better than the other three.

The singlet oxygen quantum yields (Φ_Δ) of all dyes were determined by a photochemical bleaching method[24] using 9.10-dimethylanthracene (DMA) as $^1O_2$ acceptor and $^1O_2$ phosphorescence emission at 1270 nm[13] using Rose Bengal in *n*-octanol (Φ_Δ = 1) as reference, respectively. The results are listed in Table 2 and shown in Fig. 5 and 6. The Φ_Δ of PEG-functionalized dyes are comparable with the data of BDEA, which also confirms that the terminal PEG chains have little effect on the photosensitization activity of the benzylidene cyclopentanone core. For each dye, its Φ_Δ value from the photobleaching method is relatively lower than that from the $^1O_2$ luminescence method. The latter values should be more reliable as they are taken from a direct spectroscopic measurement method.

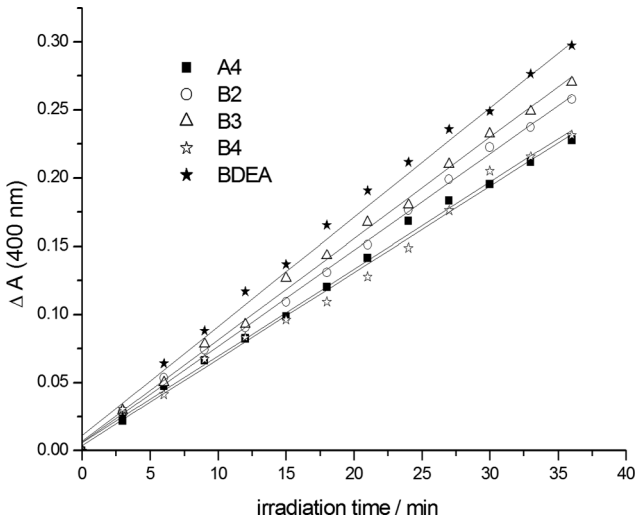

Fig. 5 Photosensitized DMA-bleaching by measuring the decrease in absorbance (ΔA) at 400 nm as a function of irradiation time in oxygen-saturated *n*-octanol solutions of dyes. The concentrations of dyes are 2×10^{-5} M. The excitation wavelength is 532 nm.

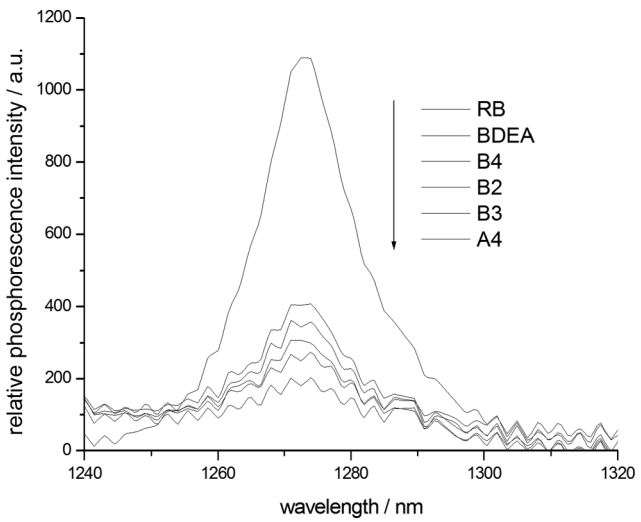

Fig. 6 Emission of singlet oxygen at 1270 nm generated by irradiating dyes in *n*-octanol with Rose Bengal (RB) as reference. The concentrations of dyes are 2×10^{-4} M. The excitation wavelength is 532 nm.

Intracellular distribution

Confocal fluorescence microscopy was used to monitor the uptake and intracellular distribution of the water-soluble dyes. Solutions of all the dyes in PBS were diluted into cell culture medium and incubated with human rectal cancer 1116 (HRC-1116) cells for

4 h. The fluorescence images of cells incubated with the dyes are shown in Fig. 7. It is clear that all dyes can taken up by HRC-1116 cells. However, their uptake ratios are different. **B2** and **B3** in cells show much stronger fluorescence compared to **A4** and **B4**, which illustrates that **B2** and **B3** are absorbed more than **A4** and **B4** by cells. This result coincides with the relatively better lipid-solubility of **B2** and **B3**.

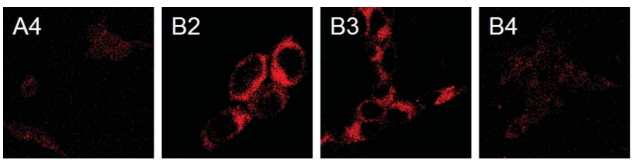

Fig. 7 Confocal fluorescence images obtained following incubations of HRC-1116 cells with 2 μg mL^{-1} dyes for 4 h. The excitation wavelength was 488 nm.

Fig. 8 shows the intracellular localization of the dyes in HRC-1116 cells after 4 h incubation, together with the localization of Mito-Tracker Green. The presence of **B2** and **B3** are evident from their red fluorescence (third column), while Mito-Tracker Green is detected by its intense green fluorescence (second column). The colocalization of dye and Mito-Tracker results in a yellow fluorescence (final column). It is clear that both **B2** and **B3** accumulate mainly in the mitochondria. No visible red fluorescence is observed in the co-staining results of **A4** and **B4** with Mito-Tracker Green, which should be due to their weak uptake.

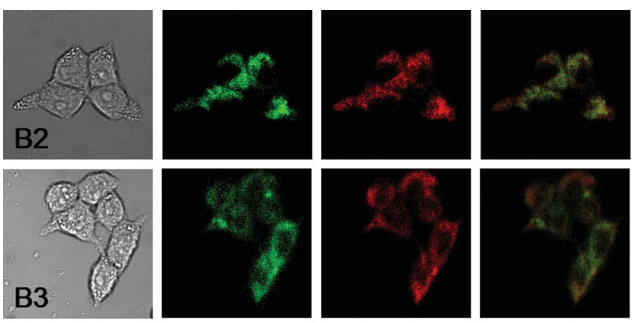

Fig. 8 Confocal fluorescence images obtained following incubations of HRC-1116 cells with 2 μg mL^{-1} dyes for 4 h and Mito-tracker green for 30 min. The excitation wavelength is 488 nm.

One- and two-photon PDT activity

For evaluating the biological PDT activity of the four water-soluble dyes (**A4**, **B2**, **B3** and **B4**) *in vitro*, PSD-007 is used as reference, which is a clinical available dye and its active ingredient is hematoporpyhrin monomethyl ether.[25] The viability of HRC-1116 cells was estimated based on measurements of MTT assay. It is shown (Fig. 9) that the four dyes all exhibit low dark toxicity (percentage of cell survival >90%), indicating that these dyes have good safety under the therapy dosage in the dark. However, only **B2** and **B3** show high phototoxicity. The possible reason is due to their optimized amphiphilicities with two PEG chains leading to higher uptake by cells compared to **A4** and **B4** with four PEG chains. It is notable that **B2** and **B3** exhibit equal or even

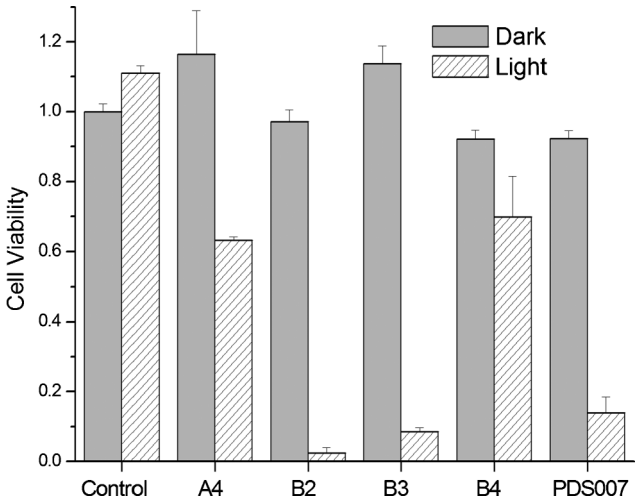

Fig. 9 Viability of HRC-1116 cells (1×10^4 cells per well) with (light) or without (dark) irradiation in the presence of dyes (10 μg mL^{-1}). The excitation wavelength is 457 nm, 20 mW cm^{-2}, 1000 s light dose (20 J cm^{-2}). The error bars denote standard deviation from three replicates.

better phototoxicity compared to PSD-007, illustrating they are promising candidates for further study in PDT applications.

The TPE-PDT experiments were also conducted on HRC-1116 cells. After a cancer cell incubated with **B3** is selectively irradiated for 5 min under focused 800 nm laser pulses (80 MHz, 80 fs) with an average power of 16 mW, a drastic hydropic degradation of the cell membrane is clearly observed (Fig. 10), while the non-irradiated cells at ambient sites remain intact. The same result is confirmed by nine replicates. Furthermore, it is very exciting to find that even under short irradiation time for 30 s and removal of light, hydropic degradation of cell can also be observed 10 min later (Fig. 11), which means that very short irradiation time is sufficient to induce cell death with TPE-PDT. Under the same condition, the degradation speed of cells incubated with **B2** is a little slower than that of cells incubated with **B3**, which may be due to their different uptake ratio by cells; this factor needs to be studied in more detail in the future. Parallel experiment without photosensitizer shows no PDT effect. The results prove the **B2** and **B3** have great potential in TPE-PDT.

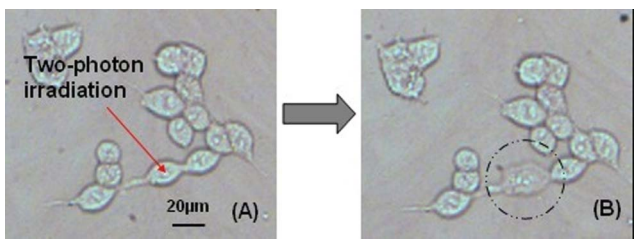

Fig. 10 Photographs of human rectal cancer 1116 cells incubated with 2 μg mL^{-1} **B3** before (A) and after (B) 5 min irradiation with 80 fs pulses at 800 nm (output power 16 mW).

Conclusions

We implemented a successful strategy to explore a series of novel PEG-functionalized benzylidene cyclopentanone dyes for TPE-PDT application. The results showed that all of them had large

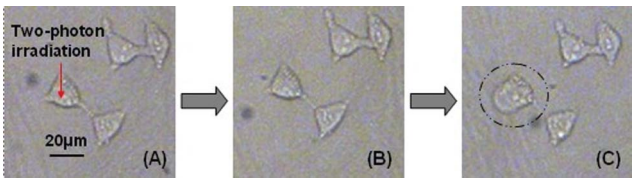

Fig. 11 Photographs of human rectal cancer 1116 cells incubated with 2 μg mL^{-1} **B3** before (A) and after (B) 30 s of irradiation, and (C) 10 min after irradiation.

TPA within 700–900 nm and high ROS yields. Among them, four dyes exhibited good solubility in PBS (>2 mg ml^{-1}, which is sufficient to clinical venous injection) and low dark toxicity under the therapy dosage. Finally, two dyes showed efficient uptake by HRC-1116 cells and were proved to have large potential in TPE-PDT application by *in vitro* cell experiments. Owing to their simple molecular structures and synthesis, we believe they will be good candidates for TPE-PDT applications in the future.

Experimental

5,5-Dimethyl-1-pyrroline-*N*-oxide (DMPO), 2,2,6,6-tetramethyl-4-piperidone (TEMP) and 9,10-dimethylanthracene (DMA) were purchased from Sigma Aldrich Chemical Company. Phosphate buffered saline (PBS) solution (pH = 7.4), Dulbecco's modified Eagle's medium (DMEM), penicillin, streptomycin, fetal bovine serum (FBS) and Mito-tracker green were purchased from Beyotime Institute of Biotechnology. 4-[*N*-methyl-*N*-(2-hycroxyethyl)amino]benzaldehyde and other materials were purchased from Beijing Chemical Co. Ltd. 4-[*N*,*N*-bis(2-hydroxyethyl)amino]benzaldehyde, 1-(*p*-tolysulfonyl)-3,6-dioxoheptane (**c1**) and 1-(*p*-tolysulfonyl)-3,6,9- trioxodecane (**c2**) were synthesized according to the literature.[26,27] Solvents used for spectroscopy experiments were spectrophotometric grade.

UV-vis spectra were recorded on a Hitachi U-3900 spectrophotometer. Steady-state fluorescence was performed using a Hitachi F-4500 spectrometer. Fluorescence quantum yields (Φ_f) were measured in dilute solutions (6×10^{-7} mol L^{-1}) using Rhodamine B in methanol as a standard ($\Phi_f = 0.7$).[28] The $^1O_2$ phosphorescence emission at 1270 nm was measured by a near infrared spectrometer (NIR-512L-1.7T1) with a 532 nm Millennia laser as light source. ^{1}H and ^{13}C NMR spectra were obtained on a Bruker DPX 400 spectrometer. The high-resolution mass spectrometry (HRMS) analyses were carried out on a Bruker apex_IV_FT mass spectrometer. Elemental analyses were performed on a Flash EA1112 elemental analyzer. The EPR signals were recorded on a Bruker ESP-300E spectrometer. All measurements were carried out at room temperature.

4-[*N*,*N*-Bis(3,6,9-trioxodecyl)amino]benzaldehyde (d1)[29]. To a stirred solution of 4-[*N*,*N*-bis(2-hydroxyethyl)amino]-benzaldehyde (2.09 g, 10 mmol) in freshly distilled THF (30 mL), KOH (2.7 g, 48 mmol) was added and the reaction mixture was refluxed for 1 h. Then, a solution of 1-(*p*-tolysulfonyl)-3,6-dioxoheptane (6.31 g, 23 mmol) in freshly distilled THF (20 mL) was added dropwise over a period of 1 h. After the addition, the reaction mixture was refluxed for 24 h. Excess solvent was neutralized by 2 M H_2SO_4 and evaporated under reduced pressure and the obtained residue was dissolved in water and extracted with CH_2Cl_2 (3 × 100 mL). The organic phase was dried over anhydrous $MgSO_4$ and rotary evaporated to give a viscous liquid, which was purified by silica gel column chromatography, elution of the column with ethyl acetate and petroleum ether mixture (1 : 1) gave a yellow viscous liquid **d1** (2.92 g, yield 72%). ^{1}H NMR (400 MHz, $CDCl_3$): δ (ppm) 3.35 (s, 6H), 3.53–3.65 (m, 24H), 6.73 (d, J = 9 Hz, 2H), 7.67 (d, J = 9 Hz, 2H), 9.70 (s, 1H).

d2–d4. A procedure identical to that described above for **d1** was utilized with different hydroxy-substituted benzaldehyde and tosylated glycol as reactants, correspondingly. **d2** (yield 75%): ^{1}H NMR (400 MHz, $CDCl_3$): δ (ppm) 3.07 (s, 3H), 3.34 (s, 3H), 3.51–3.65 (m, 12H), 6.71 (d, J = 9 Hz, 2H), 7.69 (d, J = 9 Hz, 2H), 9.70 (s, 1H). **d3** (yield 79%): ^{1}H NMR (400 MHz, $CDCl_3$): δ (ppm) 3.36 (s, 6H), 3.52–3.63 (m, 32H), 6.71 (d, J = 9 Hz, 2H), 7.66 (d, J = 9 Hz, 2H), 9.68 (s, 1H). **d4** (yield 72%): ^{1}H NMR (400 MHz, $CDCl_3$): δ (ppm) 3.09 (s, 3H), 3.36 (s, 3H), 3.52–3.68 (m, 16H), 6.73 (d, J = 8.8 Hz, 2H), 7.68 (d, J = 8.8 Hz, 2H), 9.70 (s, 1H).

2-[4-(Diethylamino)benzylidene]cyclopentanone (DEA)[18]. Cyclopentanone (8.41 g, 0.1 mol) and 4-(diethylamino)benzaldehyde (5.32 g, 0.03 mol) were dissolved in a mixed solution of ethanol (30 mL) and H_2O (10 mL) together with 0.07 g NaOH as catalyst. The reaction was performed in an ice-bath and N_2 atmosphere for 2 h and an additional 1 h at room temperature, using TLC to monitor the reaction progress. The obtained products were a mixture of mono- and di-benzylidene cyclopentanones. The desired mono-product was purified by silica gel column chromatography. Elution of the column with ethyl acetate and petroleum ether mixture (1 : 3) gave a red brown solid **DEA** (3.12 g, yield 42%). ^{1}H NMR (400 MHz, $CDCl_3$): δ (ppm) 1.19 (t, J = 7.2 Hz, 6H), 2.04 (m, 2H), 2.34 (t, 2H), 2.95 (t, 2H), 3.40 (q, J = 7.2 Hz, 4H), 6.69 (d, J = 8.5 Hz, 2H), 7.51 (d, J = 8.5 Hz, 3H).

Target dye A1. **DEA** (2.43 g, 10 mmol) and **d2** (2.81 g, 10 mmol) were dissolved in ethanol (20 mL) together with 0.06 g NaOH as catalyst. The mixed solution was refluxed in N_2 atmosphere for 8 h, then cooled to room temperature, followed by rotary evaporation to obtain the crude product. The desired dye **A1** was obtained by purification using silica gel column chromatography. Elution of the column with methanol–chloroform (1 : 50) gave deep red viscous liquid **A1** (3.27 g, yield 65%). λ_{max} (*n*-octanol)/nm (log ε) = 486 (4.80). ^{1}H NMR (400 MHz, $CDCl_3$): δ (ppm) 1.21 (t, J = 7.2 Hz, 6H), 3.05 (s, 3H), 3.07 (s, 4H), 3.37 (s, 3H), 3.43 (q, J = 7.2 Hz, 4H), 3.52–3.67 (m, 12H), 6.69 (d, J = 8.5 Hz, 4H), 7.51 (d, J = 8.5 Hz, 6H). ^{13}C NMR (400 MHz, $CDCl_3$): δ (ppm) 12.8, 26.8, 39.2, 44.6, 52.2, 59.2, 68.7, 70.8, 70.9, 71.0, 72.1, 111.3, 111.7, 123.6, 124.4, 132.8, 133.1, 133.4, 133.7, 133.8, 148.5, 149.7, 196.2. HR-MS (ESI): m/z calc. for $C_{31}H_{43}N_2O_4$ $[M + H]^+$ 507.32173; found 507.32192. Anal. Calc. for $C_{31}H_{42}N_2O_4$: C, 73.49; H, 8.36; N, 5.53. Found: C, 73.44; H, 8.39; N, 5.61%.

A2–B4 were obtained by the procedure described above. All the prepared dyes are deep red viscous liquid. The yield, NMR and HR-MS data are listed as follows: **A2** (yield 72%): λ_{max} (*n*-octanol)/nm (log ε) = 486 (4.79). ^{1}H NMR (400 MHz, $CDCl_3$): δ (ppm) 3.05 (s, 6H), 3.08 (s, 4H), 3.37 (s, 6H), 3.51–3.67 (m, 24H), 6.73 (d, J = 8.6 Hz, 4H), 7.51 (d, J = 8.6 Hz, 6H). ^{13}C NMR (400 MHz, $CDCl_3$): δ (ppm) 26.8, 39.0, 52.0, 59.0, 68.5, 70.6, 70.7, 70.8, 71.9, 111.1, 111.7, 124.1, 132.7, 133.4, 133.5, 149.6, 196.0. HR-MS (ESI): m/z calc. for $C_{35}H_{51}N_2O_7$ $[M + H]^+$ 611.36908;

found 611.36926. Anal. Calc. for $C_{35}H_{50}N_2O_7$: C, 68.83; H, 8.25; N, 4.59. Found: C, 68.91; H, 8.41; N, 4.79%. **A3** (yield 69%): λ_{max} (*n*-octanol)/nm (log ε) = 486 (4.67). ^{1}H NMR (400 MHz, $CDCl_3$): δ (ppm) 1.19 (t, J = 7.2 Hz, 6H), 3.05 (s, 4H), 3.37 (s, 6H), 3.43 (q, J = 7.2 Hz, 4H), 3.53–3.65 (m, 24H), 6.74 (d, J = 8.6 Hz, 4H), 7.52 (d, J = 8.6 Hz, 6H). ^{13}C NMR (400 MHz, $CDCl_3$): δ (ppm) 12.7, 26.7, 44.5, 51.0, 59.1, 68.5, 70.6, 70.7, 70.8, 72.0, 111.3, 111.7, 123.4, 124.3, 132.7, 132.9, 133.0, 133.2, 133.7, 133.8, 148.4, 148.5, 196.0. HR-MS (ESI): m/z calc. for $C_{37}H_{55}N_2O_7$ [M + H]$^+$ 639.40038; found 639.40072. Anal. Calc. for $C_{37}H_{54}N_2O_7$: C, 69.56; H, 8.52; N, 4.39. Found: C, 69.38; H, 8.68; N, 4.54%. **A4** (yield 73%): λ_{max} (*n*-octanol)/nm (log ε) = 488 (4.79). ^{1}H NMR (400 MHz, $CDCl_3$): δ (ppm) 3.06 (s, 4H), 3.38 (s, 12H), 3.52–3.61 (m, 48H), 6.74 (d, J = 8.5 Hz, 4H), 7.49 (d, J = 8.5 Hz, 6H). ^{13}C NMR (400 MHz, $CDCl_3$): δ (ppm) 26.7, 51.0, 59.2, 68.5, 70.7, 70.8, 70.9, 72.1, 111.7, 124.3, 132.8, 133.5, 133.6, 148.7, 196.1. HR-MS (ESI): m/z calc. for $C_{47}H_{75}N_2O_{13}$ [M + H]$^+$ 875.52636; found 875.52309. Anal. Calc. for $C_{47}H_{74}N_2O_{13}$: C, 64.51; H, 8.52; N, 3.20. Found: C, 63.92; H, 8.24; N, 3.05%. **B1** (yield 72%): λ_{max} (*n*-octanol)/nm (log ε) = 486 (4.79). ^{1}H NMR (400 MHz, $CDCl_3$): δ (ppm) 1.21 (t, J = 7.2 Hz, 6H), 3.05 (s, 3H), 3.07 (s, 4H), 3.37 (s, 3H), 3.41 (q, J = 7.2 Hz, 4H), 3.52–3.67 (m, 16H), 6.71 (d, J = 8.4 Hz, 4H), 7.51 (d, J = 8.4 Hz, 6H). ^{13}C NMR (400 MHz, $CDCl_3$): δ (ppm) 12.8, 26.8, 39.2, 44.6, 52.2, 59.2, 68.7, 70.8, 70.9, 71.0, 72.1, 111.3, 111.7, 123.6, 124.4, 132.8, 133.1, 133.4, 133.7, 133.8, 148.5, 149.7, 196.2. HR-MS (ESI): m/z calc. for $C_{33}H_{47}N_2O_5$ [M + H]$^+$ 551.34795; found 551.34846. Anal. Calc. for $C_{33}H_{46}N_2O_5$: C, 71.97; H, 8.42; N, 5.09. Found: C, 71.65; H, 8.26; N, 4.94%. **B2** (yield 72%): λ_{max} (*n*-octanol)/nm (log ε) = 487 (4.68). ^{1}H NMR (400 MHz, $CDCl_3$): δ (ppm) 3.05 (s, 6H), 3.07 (s, 4H), 3.36 (s, 6H), 3.51–3.67 (m, 32H), 6.72 (d, J = 8.5 Hz, 4H), 7.49 (d, J = 8.5 Hz, 6H). ^{13}C NMR (400 MHz, $CDCl_3$): δ (ppm) 26.8, 39.0, 52.0, 59.0, 68.5, 70.6, 70.7, 70.8, 71.9, 111.1, 111.7, 124.1, 132.7, 133.4, 133.5, 149.6, 196.0. HR-MS (ESI): m/z calc. for $C_{39}H_{59}N_2O_9$ [M + H]$^+$ 699.42151; found 699.42167. Anal. Calc. for $C_{39}H_{58}N_2O_9$: C, 67.02; H, 8.36; N, 4.01. Found: C, 66.73; H, 8.28; N, 4.06%. **B3** (yield 74%): λ_{max} (*n*-octanol)/nm (log ε) = 487 (4.80). ^{1}H NMR (400 MHz, $CDCl_3$): δ (ppm) 1.20 (t, J = 7.3 Hz, 6H), 3.05 (s, 4H), 3.37 (s, 6H), 3.41 (q, J = 7.2 Hz, 4H), 3.53–3.65 (m, 32H), 6.71 (d, J = 8.5 Hz, 4H), 7.50 (d, J = 8.5 Hz, 6H). ^{13}C NMR (400 MHz, $CDCl_3$): δ (ppm) 12.7, 26.7, 44.5, 51.0, 59.1, 68.5, 70.6, 70.7, 70.8, 72.0, 111.3, 111.7, 123.4, 124.3, 132.7, 132.9, 133.0, 133.2, 133.7, 133.8, 148.4, 148.5, 196.0. HR-MS (ESI): m/z calc. for $C_{41}H_{63}N_2O_9$ [M + H]$^+$ 727.45281; found 727.45418. Anal. Calc. for $C_{41}H_{62}N_2O_9$: C, 67.74; H, 8.60; N, 3.85. Found: C, 67.29; H, 8.43; N, 3.74%. **B4** (yield 61%): λ_{max} (*n*-octanol)/nm (log ε) = 486 (4.70). ^{1}H NMR (400 MHz, $CDCl_3$): δ (ppm) 3.06 (s, 4H), 3.38 (s, 12H), 3.52–3.61 (m, 64H), 6.74 (d, J = 8.7 Hz, 4H), 7.49 (d, J = 8.7 Hz, 6H). ^{13}C NMR (400 MHz, $CDCl_3$): δ (ppm) 26.7, 51.0, 59.2, 68.5, 70.7, 70.8, 70.9, 72.1, 111.7, 124.3, 132.8, 133.5, 133.6, 148.7, 196.1. HR-MS (ESI): m/z calc. for $C_{55}H_{91}N_2O_{17}$ [M + H]$^+$ 1051.63122; found 1051.63098. Anal. Calc. for $C_{55}H_{90}N_2O_{17}$: C, 62.84; H, 8.63; N, 2.66. Found: C, 62.33; H, 8.51; N, 2.72%.

Solubility and lipid-water partition coefficient. To determine the maximum solubility in PBS, absorption spectra for photosensitizer dissolved in PBS solution in a series of concentrations were measured. The top value at absorption band maximum in the linear range of the plot was recognized to be the maximum solubility. For experiments of determining the partition coefficient (PC), photosensitizers were diluted to a concentration of 20 μM in 2 mL PBS (PH = 7.4), and then 2 mL *n*-octanol was added. The mixture of the two solvents was vigorously stirred and sonicated for 2 min, then centrifuged at 4000 rpm for 10 min to separate the phases. The photosensitizer concentrations in *n*-octanol phase and PBS phase were determined by UV spectroscopy. Then the final lipid-water PC values were calculated by the ratio of photosensitizer concentration in *n*-octanol to that in PBS solution.

EPR experiments. Experimental details are as follows, microwave bridge: X-band with 100 Hz field modulation; sweep width: 100 G; modulation amplitude: 1.0 G; modulation frequency, 100 kHz; receiver gain: 1×10^5; microwave power: 5 mW. Samples were purged with oxygen for 15 min in the dark, and then injected into the specially made quartz capillaries for EPR analyses. According to the experimental requirement, samples were illuminated directly in the cavity of the EPR spectrometer with a Nd:YAG laser (532 nm, 5–6 ns of pulse width, repetition frequency: 10 Hz, 10 mJ/pulse energy). The kinetics of spin adduct generation were studied by recording peak heights of EPR spectra every 40 s. DMPO and TEMP were used as superoxide radical and singlet oxygen spin-trapping reagent, respectively. The solution components were as follows: 100 μL dye (1×10^{-4} M) plus 3 μL pure TEMP or 20 μL 0.2 M DMPO. The solvents were DMSO and toluene, respectively.

Singlet oxygen quantum yield. In the photochemical method, 9.10-dimethylanthracene (DMA) was used as $^1O_2$ acceptor. A 532 nm diode laser was used as the light source. Dyes and DMA were dissolved in *n*-octanol and saturated with oxygen in the dark. The concentrations of all the photosensitizers were adjusted to possess the same absorbance at 532 nm. Experiments were performed by monitoring the bleaching of the absorption band of DMA at 400 nm as a function of the irradiation time. The slope of the curves obtained was an indication of the efficiency to generate singlet oxygen (the larger the slope, the better the efficiency). Additionally, three control experiments: 1, no irradiation; 2, no photosensitizer; and 3, aerate with N_2 to remove O_2, were performed, none of these experiments resulted in any absorbance changes in the reaction mixture, which proved that the generation of singlet oxygen was an integrative action with three components: photosensitizer, light and oxygen, none is dispensable. In the $^1O_2$ phosphorescence method, samples in *n*-octanol were prepared with a concentration of 2×10^{-4} M. A 532 nm diode laser was used as the light source. A near infrared fiber spectrometer (NIR-512L-1.7T1) was used as monitor. Rose Bengal (RB) in *n*-octanol was used as a reference standard with $\Phi_\Delta = 1$.

TPA characterization. TPA cross-section (σ) values of compounds in *n*-octanol (2×10^{-4} M) were determined using the two-photon excited fluorescence (TPEF) technique following the experimental protocol described in detail by Xu and Webb.[30] The excitation light sources were a mode-locked Tsunami Ti : sapphire laser (720–880 nm, 80 MHz, <130 fs). Two-photon excited fluorescence spectra were recorded in a direction perpendicular to the laser beam using a fiber spectrometer (Ocean Optics USB2000 CCD) as detector. Rhodamine B in methanol solution (10^{-4} M) was used as reference. To avoid any contribution from other photophysical or photochemical processes, the intensity of input

pulses were adjusted to a appropriate regime to ensure a quadratic dependence of the fluorescence intensity *vs*. excitation pulse energy (shown in Fig. S1, ESI†).

Cell culture. HRC-1116 cells were grown in culture media of DMEM supplemented with 100 unit/ml penicillin, 100 μg ml^{-1} streptomycin and 10% FBS at 37 °C in a humidified atmosphere containing 5% CO_2.

Confocal fluorescence images. Dye stock solutions (1 mg ml^{-1}) were prepared in PBS and then diluted into final working concentrations. HRC-1116 cells were seeded in a two-well coverglass chamber at a density of 2×10^5 cells per well in culture media. After 24 h, the culture media was replaced with medium containing 2 μg mL^{-1} dyes and incubated for 4 h. Following incubation, the chambers were washed twice with PBS to remove free dyes. Then the cells were incubated with the medium containing fluorescent tracker for 30 min. After carefully washing with PBS twice again, imaging was performed using a confocal laser scanning microscope (Nikon Eclipse C1Si), coupled to a CW argon-ion laser (488 nm). A dry 40× (NA = 0.75) objective was used for imaging.

One-photon PDT model. HRC-1116 cells were plated in flat-bottomed 96-well plates of 10^4 cells per well in culture medium for 24 h. The medium was replaced with culture medium containing 10 μg mL^{-1} photosensitizer and the cells were then incubated in the dark for 4 h followed by irradiation under a 457 nm diode laser (20 mW cm^{-2}) for 1000 s. The control group without photosensitizer was treated with a 457 nm laser and taken as a 100% cell survival base line. After irradiation, the cells were incubated in the dark for 24 h before survival assessment. The cell deaths were determined based on the cell survival as estimated by MTT assay.[31]

Two-photon PDT model. HRC-1116 cells were seeded in a two-well coverglass chamber at a density of 2×10^5 cells per well in culture media. After 24 h, the culture media was replaced with medium containing 2 μg mL^{-1} dye and incubated for 4 h followed by irradiation under a mode-locked femtosecond Ti : sapphire laser (Tsunami Ti: sapphire, 800 nm, 80 MHz, 80 fs) through an objective (10×, NA = 0.4, Olympus). The sample was fixed on an *xyz*-step motorized stage controlled by a computer. Before illumination, the focused laser point was adjusted to the middle of a target cell. The illumination intensity was 16 mW.

Acknowledgements

This work was supported by the National Natural Science Foundation of China (No. 60978057). The authors are grateful to Dr Hongyan Zhang for her expertise assistance with the confocal fluorescence microscopy.

Notes and references

1 T. J. Dougherty, C. J. Gomer, B. W. Henderson, G. Jori, D. Kessel, M. Korbelik, J. Moan and Q. Peng, *J. Natl. Cancer Inst.*, 1998, **90**, 889.
2 D. E. Dolmans, D. Fukumura and R. K. Jain, *Nat. Rev. Cancer*, 2003, **3**, 380.
3 H. I. Pass, *J. Natl. Cancer Inst.*, 1993, **85**, 443.
4 J. D. Bhawalkar, N. D. Kumar, C. F. Zhao and P. N. Prasad, *J. Clin. Laser Med. Surg.*, 1997, **15**, 201.
5 K. Ogawa and Y. Kobuke, *Anti-Cancer Agents Med. Chem.*, 2008, **8**, 269.
6 A. Karotki, M. Khurana, J. R. Lepock and B. C. Wilson, *Photochem. Photobiol.*, 2006, **82**, 443.
7 M. Khurana, H. A. Collins, A. Karotki, H. L. Anderson, D. T. Cramb and B. C. Wilson, *Photochem. Photobiol.*, 2007, **83**, 1441.
8 H. A. Collins, M. Khurana, E. H. Moriyama, A. Mariampillai, E. Dahlstedt, M. Balaz, M. K. Kuimova, D. Phillips, M. Drobizhev, A. Rebane, B. C. Wilson and H. L. Anderson, *Nat. Photonics*, 2008, **2**, 420.
9 E. Dahlstedt, H. A. Collins, M. Balaz, M. K. Kuimova, M. Khurana, B. C. Wilson, D. Phillips and H. L. Anderson, *Org. Biomol. Chem.*, 2009, **7**, 897.
10 K. Ogawa and Y. Kobuke, *Org. Biomol. Chem.*, 2009, **7**, 2241.
11 S. C. Boca, M. Four, A. Bonne, B. von der Sanden, S. Astilean, P. L. Baldeck and G. Lemercier, *Chem. Commun.*, 2009, 4590.
12 K. D. Belfield, M. V. Bondar, F. E. Hernandez, A. E. Masunov, I. A. Mikhailov, A. R. Morales, O. V. Przhonska and S. Yao, *J. Phys. Chem. C*, 2009, **113**, 4706.
13 M. Velusamy, J. Y. Shen, J. T. Lin, Y. C. Lin, C. C. Hsieh, C. H. Lai, M. L. Ho, Y. C. Chen, P. T. Chou and J. K. Hsiao, *Adv. Funct. Mater.*, 2009, **19**, 2388.
14 S. Kim, T. Y. Ohulchanskyy, H. E. Pudavar, R. K. Pandey and P. N. Prasad, *J. Am. Chem. Soc.*, 2007, **129**, 2669.
15 C. Y. Chen, Y. Q. Tian, Y. J. Cheng, A. C. Young, J. W. Ka and A. K. Y. Jen, *J. Am. Chem. Soc.*, 2007, **129**, 7220.
16 J. Wu, Y. X. Zhao, X. Li, M. Q. Shi, F. P. Wu and X. Y. Fang, *New J. Chem.*, 2006, **30**, 1098.
17 J. Q. Xue, Y. X. Zhao, J. Wu and F. P. Wu, *J. Photochem. Photobiol., A*, 2008, **195**, 261.
18 J. Wu, M. Q. Shi, Y. X. Zhao and F. P. Wu, *Dyes Pigm.*, 2008, **76**, 690.
19 R. B. Greenwald, Y. H. Choe, F. McGuire and C. D. Conover, *Adv. Drug Delivery Rev.*, 2003, **55**, 217.
20 S. K. Sahoo, T. Sawa, J. Fang, S. Tanaka, Y. Miyamoto, T. Akaike and H. Maeda, *Bioconjugate Chem.*, 2002, **13**, 1031.
21 J. Y. Liu, X. J. Jiang, W. P. Fong and D. K. P. Ng, *Org. Biomol. Chem.*, 2008, **6**, 4560.
22 N. Cauchon, H. J. Tian and R. Langlois, *Bioconjugate Chem.*, 2005, **16**, 80.
23 B. W. Henderson, D. A. Bellnier, W. R. Greco, A. Sharma, R. K. Pandey, L. A. Vaughan, K. R. Weishaupt and T. J. Dougherty, *Cancer Res.*, 1997, **57**, 4000.
24 Y. Zhang, J. Xie, L. Y. Zhang, C. Li, H. X. Chen, Y. Gu and J. Q. Zhao, *Photochem. Photobiol. Sci.*, 2009, **8**, 1676.
25 X. M. Ding, Q. Z. Xu, F. G. Liu, P. K. Zhou, Y. Gu, J. Zeng, J. An, W. Dai and Z. S. Li, *Cancer Lett.*, 2004, **216**, 43.
26 A. W. Snow and E. E. Foos, *Synthesis*, 2003, 509.
27 A. W. Harper, S. S. H. Mao, Y. Ra, C. Zhang, J. Zhu and L. R. Dalton, *Chem. Mater.*, 1999, **11**, 2886.
28 J. N. Demas and G. A. Grosby, *J. Phys. Chem.*, 1971, **75**, 991.
29 T. A. Kalliat and R. Danaboyina, *J. Phys. Chem. A*, 2005, **109**, 5571.
30 C. Xu and W. W. Webb, *J. Opt. Soc. Am. B*, 1996, **13**, 481.
31 A. M. R. Fisher, K. Danenberg, D. Banerjee, J. R. Bertino, P. Danenberg and C. J. Gomer, *Photochem. Photobiol.*, 1997, **66**, 265.